Evaluation of Blast Mitigation Capability of Advanced Combat Helmet by Finite Element Modeling

Sumit Sharma, Rahul Makwana, Liying Zhang, Ph.D

Wayne State University, Detroit, MI, USA

Abstract

Primary blast wave induced traumatic brain injury and posttraumatic stress disorders have been observed in great number among military personnel in the recent Iraq and Afghanistan wars. Although combat helmets provide good protection against blunt/ballistic type threats, the current issue with military helmets is protection concerning the threats from primary blast wave. This study focused on investigating how combat helmets influence the blast-induced biomechanical loads in the human brain. Multi-Material Arbitrary Lagrangian Eulerian method was applied to simulate the wave propagation in the shock tube, the interaction of the shock wave with the human head, and the subsequent blast overpressure transformation through the head.

The finite element model (FE) of Wayne State University shock wave generator (WSUSG) was developed and validated against experimentally measured side-on pressure time histories within the tube. Validated 3-D FE models of the human head and Advanced Combat Helmet (ACH) reported previously were used to predict the internal brain responses and assess the performance of the helmet in mitigating shock wave of various severities generated by WSUSG. Effectiveness of helmet with respect to various head orientations to oncoming shock waves was also evaluated. Biomechanical response parameters including the peak brain pressures and strains at various regions of the brain were calculated and compared between the heads with and without helmet.

Wearing ACH was found to mitigate the intracranial pressures up to 33% at given blast loading conditions. The peak brain strain was reduced by 13-40% due to the use of helmet. In generally, ACH exhibited increased protective performance as the shock intensity increased. The current ACH helmet design offered superior protection to the brain in sideways blast than that in forward blast loading condition of same severity.

1. Introduction

Blast induced traumatic brain injury (bTBI) has been recognized as a "signature injury" in the recent Iraq and Afghanistan wars [1]. It was estimated that among thousands of U.S. soldiers have sustain traumatic brain injury (TBI), about 70% was resulted from blast injury [2-3]. Department of Defense Armed Forces Health Surveillance Center (AFHSC) reported that a total of 229,106 of the service members have been diagnosed with TBI between 2000 and the third quarter of 2011, with over 75% of these cases being of mild TBI without any overt physical or visible brain damage by imaging [4].

Combat helmets remain to be the primary equipment of protection for warfighters. The effect of primary blast wave on brain injury resulting from Improvised Explosive Devices (IEDs) has not been addressed in the current combat helmet design. Recently, both protective and un-protective effects of a combat helmet against blast loadings have been proposed by a number of research groups [5-8]. However, most of these computer models used were either purely descriptive or lacked detailed geometrical and material characteristics of the head and helmet system. Furthermore, none of the FE head model applied has been validated against intracranial responses measured in the cadaveric brain exposed to blast loadings.

This communication was to report a finite element (FE) study conducted in order to understand the blast effects on the human head and how combat helmets influence the blast-induced biomechanical loads in the brain. Multi-Material Arbitrary Lagrangian Eulerian (MMALE) method in LS-DYNA (LSTC, Livermore) was applied to simulate the wave propagation in the shock tube, the interaction of the shock wave with the human head, and the subsequent blast overpressure transformation through the head. A sophisticated FE human head model previously developed and validated against cadaveric intracranial pressure measurements in shock tube experiments [9, 10]was used and integrated with a detailed, validated FE advanced combat helmet (ACH) model. The peak pressures and strains within the brain tissue of various regions in response to a variety of blast loading severities and directions were compared to assess blast wave mitigation capability of the combat helmet used by the U.S. Army service members.

2. Materials and Methods

2.1 FE Models

Human head model
The sophisticated FE human head model, Wayne State University Head Injury Model (WSUHIM) [9, 11-12] was utilized for the study. This high resolution FE model features fine anatomical details including scalp, skull with an outer table, dipole and an inner table, cerebral meninges (dura, falx, tentorium), arachnoid, CSF, pia mater hemispheres of the cerebrum with distinct white and gray matter, cerebellum, brainstem, lateral and third ventricles, and bridging veins for cranial part (Figure 1). The entire head model was made up of over 330,000 elements and uses 15 different material properties and constitutive models for various tissues in the head. Human brain was defined as nearly incompressible viscoelastic material [9, 20-21]. The head model has been subjected to rigorous validations against available experimentally measured intracranial pressure, ventricular pressure, brain/skull relative motion and facial impact responses obtained from cadaveric dynamic impact tests [13-17].
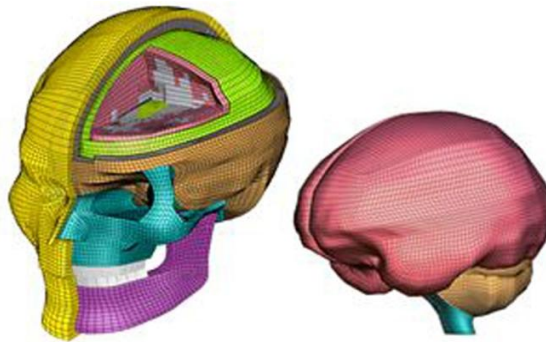

Figure 1: An anatomically accurate FE model of the human head (WSUHIM)

Combat helmet model
A detailed 3D FE model of the ACH was developed based on surface geometry of an actual helmet scanned using a 3-D digital scanner. The current ACH helmet has a 10 mm thick shell with pad system configuration consisting of seven pads in three different shapes. The mesh of the seven pads included two-part foams (impact and conform liners) with a thickness of about 10 mm for each. The entire helmet model consisted of over 81,000 elements with an average element size of approximately 2-3 mm (Figure 2). The integrated FE models of the ACH and a

mid-size Department of Transportation (DOT) headform were validated against headform acceleration measured from U.S. Army blunt impact experiments conducted on ACH [19, 31, 33].
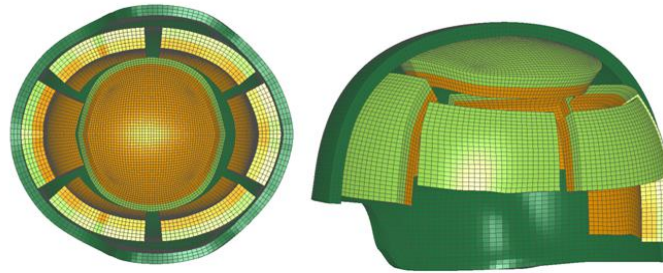

Figure 2: 3D FE ACH model: bottom view and side view with half of shell removed to expose the padding system

MAT_COMOSITE_DAMAGE (MAT_22) was chosen to model the woven fabric reinforced aramid laminates of the ACH shell. This material model allows assignment of different material properties to the fibers in three orthogonal directions (a, b, and c).According to literature, two directions in fabric reinforced aramid laminates of shell had similar material behaviors [22]. Therefore, a transversely isotropic material would be sufficient to define the material behavior of the ACH shell. The material parameters for the shell material (Table 2) were based upon the data reported in literature [23-24].

Table 1: Material parameters defined for woven fabric aramid laminates of the ACH shell

Density (kg/mm^3)	Young's Modulus Ea (GPa)	Young's Modulus Eb (GPa)	Young's Modulus Eb (GPa)	Poisson's Ratio (vba)
1.23x10^{-6}	18.5	18.5	6	0.25
Poisson's Ratio (vba)	Poisson's Ratio (vba)	Shear Modulus G_{ab} (GPa)	Shear Modulus G_{bc} (GPa)	Shear Modulus G_{ca} (GPa)
0.33	0.33	0.77	2.72	2.72

ACH utilizes a ZAP^{TM} (Zorbium Action Pad) padding systems for impact and comfort liners that are polyurethane-based foam materials exhibiting loading-rate dependent stress-strain behavior. The material properties for the two foams were obtained from standard ASTM material testing provided by Team Wendy LLC (Cleveland, OH) [25], the sole manufacturer and supplier of impact absorbing systems for ACH since 2005. The uniaxial compression tests were conducted at strain rates of 0.02, 0.2, 2, 20 and 200 s^{-1} to a normal strain of 80%. The densities of the hard and soft foams were 6.1 x 10^{-8} and 6.3 x 10^{-8} kg/mm^3 respectively. The material behaviors of the two foams were modeled by adopting MAT_LOW_DENSITY_FOAM (MAT_57). The elastic moduli of the hard (8.4 MPa) and soft foams (0.840 MPa) were used as reference moduli along with a decay constant of 5 ms^{-1}. Stress strain data obtained at the highest strain rate (200 s^{-1}) from the two foams were selected.

Head and helmet model integration
The positioning of the ACH on the WSU head model was defined properly according to the basic guidelines and instructions in the ACH technical manual [29] (Figure 3). A surface to surface

contact definition together with a coefficient of friction of 0.3 was defined at the interface between the head skin and helmet padding surface to represent a solider wearing helmet. The integrated head/helmet model was applied previously to simulate helmet drop tests and compared to measured tests data [31, 33].
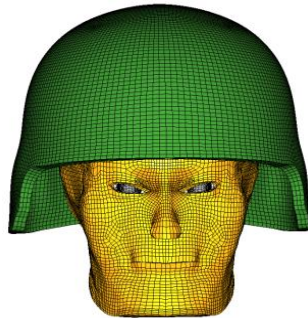

Figure 3: Integrated FE models of ACH and WSUHIM

WSUSG model

Shock tube (also called shock wave generator) is basically a cylindrical hollow object with strong boundary to create a shock wave, with similar characteristics of blast wave generated in open-field. Figure 4a shows the Wayne State University Shockwave Generator (WSUSG). As shown in Figure 4b (FE model), driven segment is the longest part and contains air at ambient pressure initially. Driver and Driven compartments are separated by a Mylar membrane. With the rupture of this membrane, highly compressed air from Driver suddenly travels through the Driven and behaves like blast waves. The rupture point of the Mylar tube is defined by its thickness and it controls the incident shock overpressure near the head. To create high pressure shock waves, thicker Mylar membrane is used so that it requires higher pressure in the Driver for rupture [26-27].
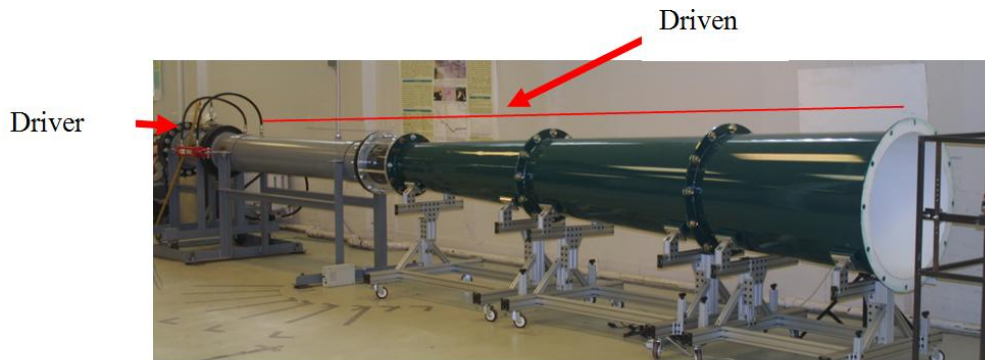
(a)
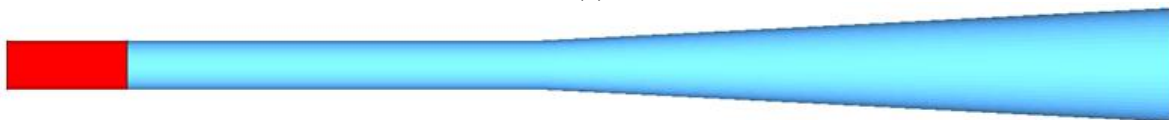
(b)
Figure 4: (a) Wayne State University Shockwave Generator (WSUSG), (b) FE model of WSUSG

Coupled MMALE algorithm was adapted to model driver, driven, the formation of the shockwaves and wave flow within the WSUSG. Air and helium were assigned by *MAT_NULL

with linear polynomial equation of state [28]. The polynomial equation of state can be described as:

$$P = C_0 + C_1\mu + C_2\mu^2 + C_3\mu^3 + \left(C_4 + C_5\mu + C_6\mu^2\right)E.$$

Where $C_0 = C_1 = C_2 = C_3 = C_6 = 0$ and $C_4 = C_5 = \gamma - 1$, γ is the ratio of specific heat that is 1.4 for air and 1.66 for helium.

2.5 Shock Wave Loadings on Head and Helmeted Head models

Shock tube pressure validation
Figure 5 (a) shows the sketch of the shock tube with the locations of three pressure sensors at Driver (A_c), Rwall (B_c) and additional lollipop pressure sensors (C_c) near to the cadaver head inside the shock tube to capture the pressure time histories during shock. The real-time recorded pressure sensor data at Rwall and side-on were used to validate the FE WSUSG model. Four pressure sensors were placed within the cadaver brain to capture the intracranial pressure responses. Each sensor location was identified in the FE head model for the frontal, parietal and occipital lobes (30 mm in depth) and the ventricle (60 mm in depth) region as shown in Figure 5 (b).The model predicted ICP results were compared to the measured senor data to validate the head model.

Effect of helmet on brain responses from forward blast of various severities
The head model and the helmet-head model were subjected respectively to a forward shock wave exposure (Figure 5c) of varying intensities. The peak overpressures of 170 and 300 kPa in addition to 71 kPa were simulated. The desired incident overpressure intensities were achieved by varying the compression pressures in the driver chamber. The nomenclature of the cases was made based on the direction and peak intensity of the shock waves, i.e. forward Case_71kPa.

Directional effect of helmeted head and bare head
Blast mitigation capability of ACH was further assessed by changing the orientations of the head and helmeted-head models from forward facing to sideways toward the oncoming shock wave traveling in the shock tube. For each of the loading conditions, the peak intracranial pressure and strain responses at different brain locations between the heads with and without helmet were compared to evaluate the role of a combat helmet in mitigating the blast effect.
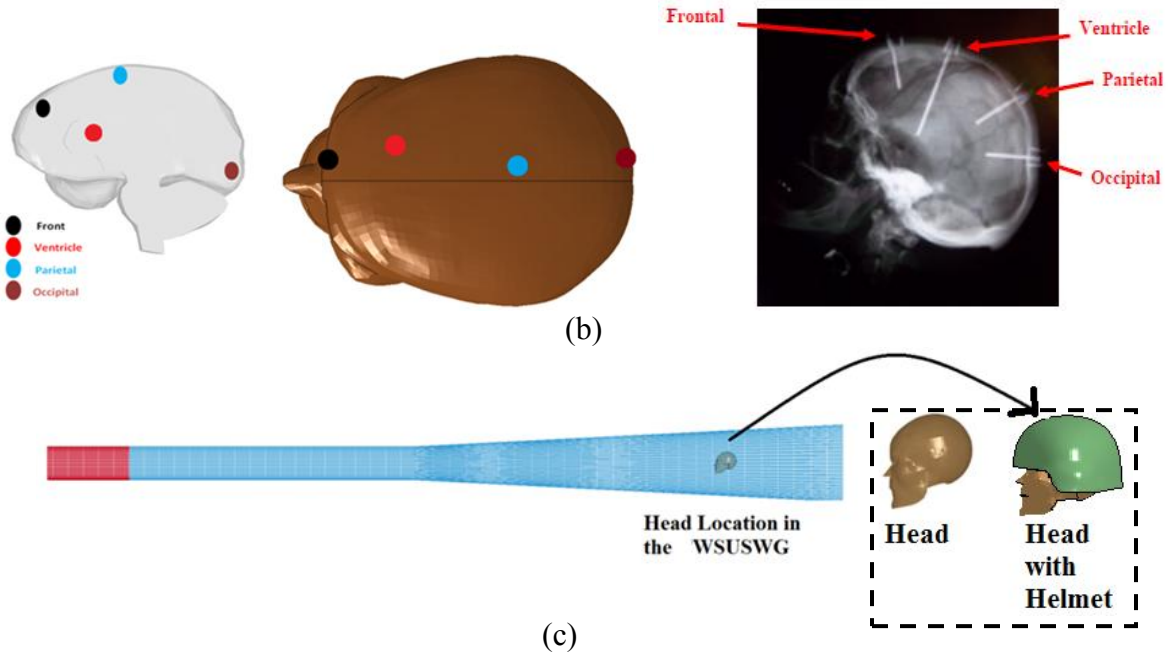

(a)

(b)

(c)
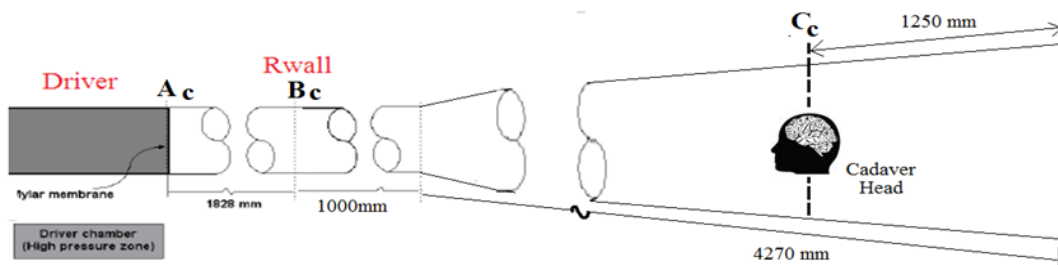
Figure 5: Schematic drawings and FE models depict: (a) Dimensions of the WSUSG with positioning of the cadaver head used in the experiments and X ray of cadaver 4 [35], (b) The locations of the elements defined for output of the pressure responses in the FE head model that were in accordance with the locations of pressure transducers mounted in the cadavers brain, and (c) FE model setup for simulating the forward shock experiments with and without a helmet

3. Results

3.1 Model Validation
WSUSG and WSU head model
Figure 6 shows the comparison of the overpressure time histories obtained at two locations within shock tube between the model predictions and pressure sensor measurements for forward Case_71kPa. The model results agreed with the sensor data in terms of peak pressure magnitude and overall pulse duration, except the model under-predicted secondly peak at 5 ms before the decay of the overpressure. The WSUSG model was also validated for higher incident shock intensity cases (76, 104 kPa) and had good correlations between the numerical and experimental results.
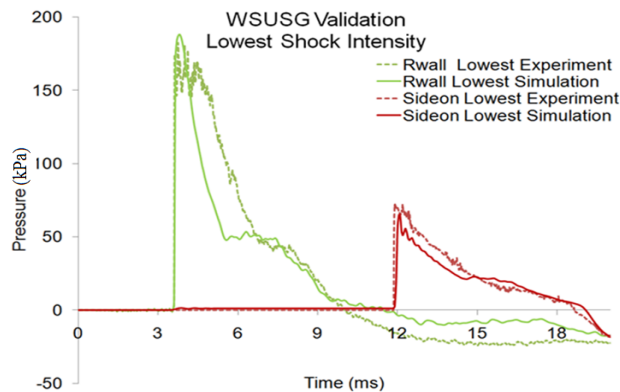

Figure 6: Validation of the pressure time histories for forward shock case_71kPa, at RWall and Side-on locations

Figure 7 shows the comparison of the intracranial pressure time histories between head model simulations and cadaveric experimental measurements at four brain locations in forward Case_71 kPa. In the front cortical region, the general brain pressure history patterns were similar between experimental and simulation results. The peak magnitude in the coup cortex however, was under-predicted by the FE model. Ventricular pressure predicted by the model fell well in the range of the results between the two cadavers. The peak tensile pressures at the occipital region for all three intensities were found in line with the peak values of two cadaver's data. The change of pressure from negative to positive in occipital regions seemed to occur earlier in model simulations than in experiments. More cadaver experimental data are needed to fully validate the head model.
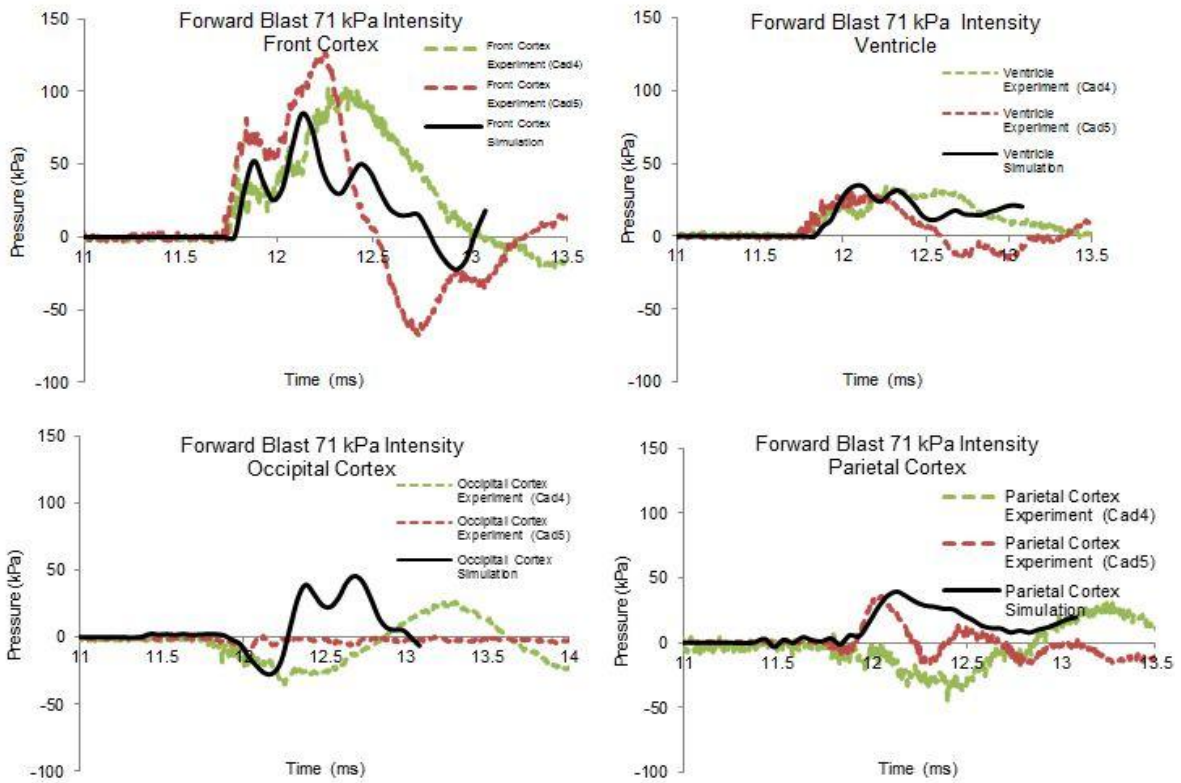

Figure 7: Validation of the ICP time histories at the frontal, parietal, ventricular, and occipital regions as a result of low intensity forward blast generated by WSUSG

3.2 Brain Response Comparison between the Heads with and without Helmet

Intracranial pressure
The intracranial pressure (ICP) time histories predicted by the two models at various brain locations for forward Case_71kPa are shown in Figures8 a, b. It can be seen clearly that the magnitudes as well as the patterns of ICP were significantly affected by the presence of the helmet. Both cases showed the coup and countercoup phenomena. With the helmet, peak positive and negative pressures were reduced to from 87 kPa (coup) to 61 kPa and from -34 kPa (contrecoup) to -24 kPa, respectively. The ventricle and parietal cortex also experienced reduced pressure with the presence of helmet (Figures8c). The ICP reduction ranged from 10 to 28%with

the highest on the coup site (Figure 8c). Figure 9 shows the pressure contour patterns peaked throughout the sagittal plane of the head with and without helmet in use.

(a)   (b)   (c)
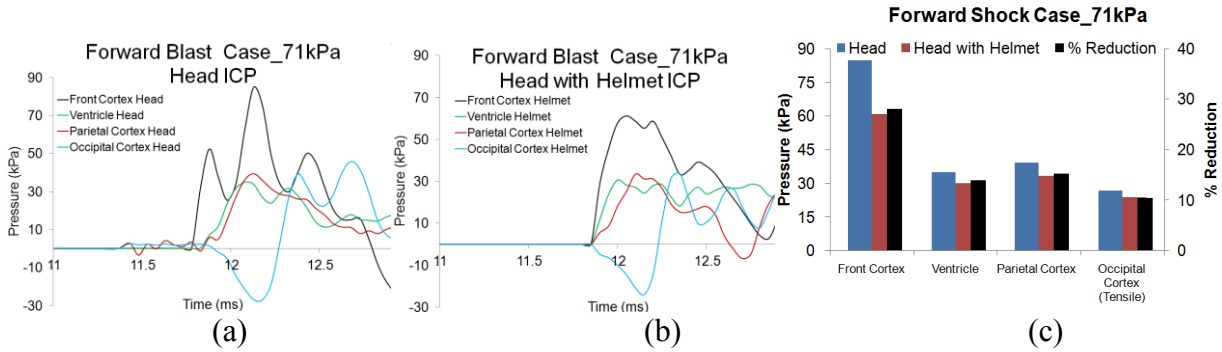
Figure 8: Intracranial pressure time histories monitored for various brain regions (a) without and (b) with helmet in forward Case_71kPa, and (c) Peak intracranial pressure comparison and reduction in various brain locations in forward shock cases
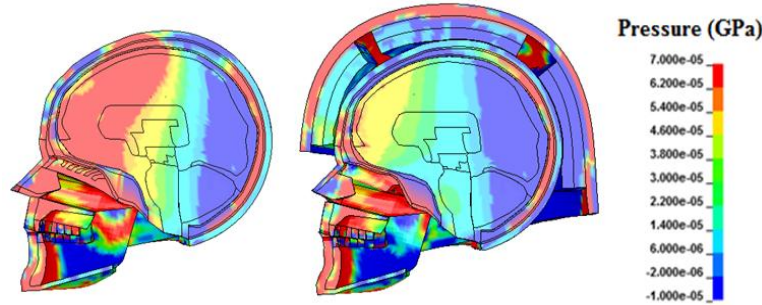

Figure 9: Peak intracranial pressure contour patterns throughout the sagittal plane of the head without and with helmet in forward shock loadings

Brain strain
Figure 10 compares the peak magnitudes of the maximum principal strain sustained in the brain at various regions between the heads with and without helmet in forward Case_71kPa. Overall, wearing a helmet reduced the strain in the brain by 13% - 40% depending on the regions at given loading severity. The overall strain magnitudes were below 0.004 and 0.01 respectively, with and without helmet in use.
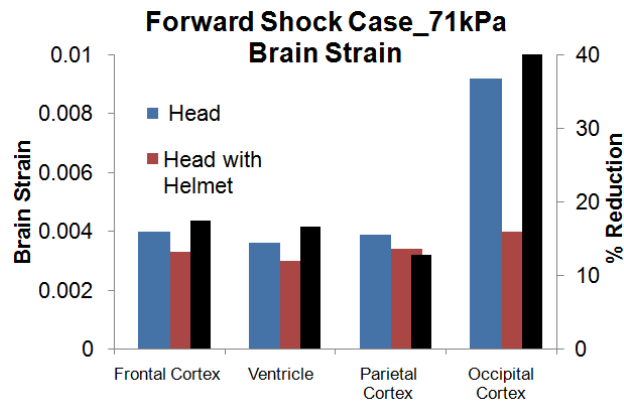

Figure 10: Peak intracranial strains in the brain locations for without and with helmet forward shock cases

3.3 Performance of the Helmet under Higher Shock Intensities

Under higher incident pressures of 170 and 300 kPa, the resulting intracranial pressures predicted in the brain showed similar temporal profiles to that of Case_71 kPa described above. As the incident overpressure in the shock tube increased from 71 to 300 kPa, the resulting highest brain coup pressure increased from 85 to 620 kPa for non-helmeted head and from 61 to 350 kPa for helmeted head. The degrees of ICP changes at various regions of brain varied depending on the blast loading severities and whether helmet was in use or not. It was interesting to note that at higher shock intensity, the helmet exhibited increased efficiency in mitigating the blast effect in the brain (43% reduction) than at lower blast loading condition (28% reduction) (Figure 11).
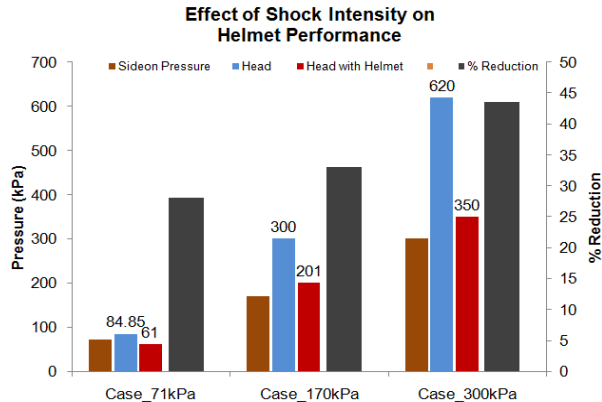

Figure 11: Peak intracranial pressures comparison in the coup brain regions for helmet and without helmet cases in forward shock of higher intensities

3.4 Performance of Helmet in Sideways Shock

Figure 12a compares the peak ICP at different brain locations between the head with and without helmet during a sideway shock Case_71kPa. Like in forward shock case, helmeted head had reduced intracranial pressure in sideway shock. Peak pressure reductions varied by regions ranging from13 to 33% with the highest reduction in the coup site. Figure 12b compares the performance of helmet in mitigating the ICP responses in forward and sideway shock. It can be seen clearly that the helmet performed better in sideway shock as compared to forward shock loading in terms of reducing the ICP throughout different regions of the brain.
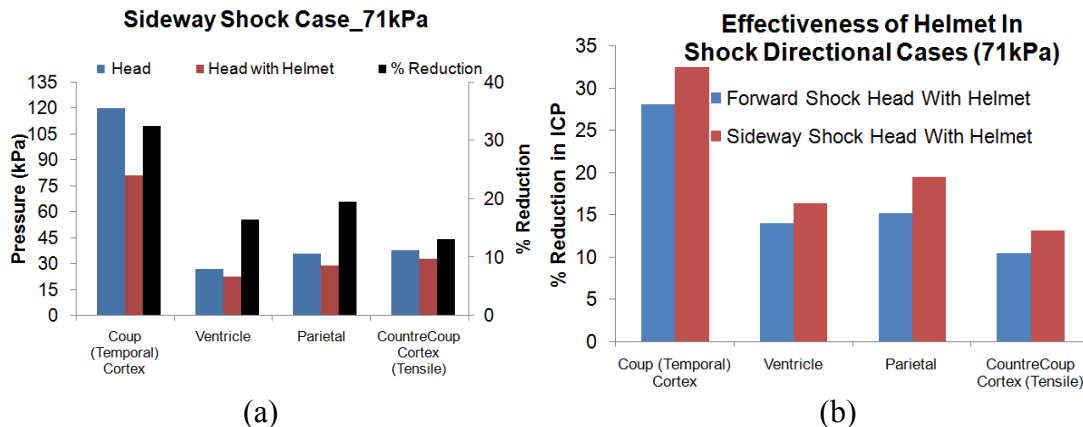

(a)

(b)

Figure 12: (a) Peak brain pressure comparison in various brain locations with and without helmet in sideway shock, and (b) Helmet effect between forward and sideways shock

4. Discussions and Conclusions

This study was performed to comprehend the biomechanical effects of shock wave on human brain and to evaluate the blast mitigation performance of the current military helmet under various blast loading conditions. A number of FE models applied including an anatomically detailed human head, advanced combat helmet, WSU shock generator which were previously extensively validated against blunt impact conditions. In the current study, the WSUHIM was further validated against experimentally measured cadaveric intracranial pressure in blast loading condition, which has never been reported before. The validated head model coupled with ACH helmet model was applied successfully to capture the impinge of shock wave generated from shock tube on the head/helmet structure and subsequent wave transformation process through the helmet to brain during blast insults of varying intensities and directions. The hybrid Lagrangian-Eulerian algorithm approach utilized appeared to be a useful tool for simulating blast wave phenomena in the shock tube, fluid-solid coupling and subsequent brain structure responses to blast loads [30-32]. The further validation of the head model in blast loading conditions is required when more cadaveric experimental data become available both from shock tube and open field tests.

In forward shock, the helmet shell was pushed onto the head as the helmet pads deformed from blast loading. It was also observed that small portion of the blast wave directly entered through the gap between the helmet and the forehead causing additional deformation on the surrounding pads. Overall, ACH helmet was found to lower the resulting intracranial pressures and brain strains induced by the blast wave in comparison with head without a helmet. It was also noticed that percentage reduction in resulting brain pressure in helmeted head was 28%in forward Case_71kPa where as it was up to 45% in Case_300kPa. This suggested that the current ACH helmet was more efficient in mitigating the shock wave from blast threats of relatively higher intensity than the lower intensity shock.

In case of without helmet, the intracranial pressure response in the brain induced by the sideways shock was more than 35% higher than that produced by the forward shock, suggesting a relatively high risk for sustaining blast wave induced TBI when the side of head is directly facing the oncoming shock wave. This directional dependency of brain responses to blast wave was also observed from open-field blast cases reported in our previous study [9, 30-31]. The decreased brain tolerance to lateral loading was in consistent with findings reported for brain trauma in blunt impact [34]. The present investigation showed that current combat helmet provided better protection in sideways blast (33%) than in frontal blast (28%). The increased projected area in the side of the helmet compared to the areas in the front may result in greater protection to the side of the head [33]. However, the overall biomechanical responses sustained by the brain remained to be higher from a sideways shock than that from a frontal shock. Thus, direction-specific tolerances need to be determined and applied in helmet design in order to offer omni-directional protection for the human head in combating blast induced TBI [31].

Acknowledgements

References

1. Cernak I., and Nobel-Haeusslein L. J. Traumatic brain injury: an overview of pathobiology with emphasis on military populations. J Cereb. Blood Flow Metab 30 (2009) 255-266.
2. Fischer H. United States Military Casualty Statistics: Operation Iraqi Freedom and Operation Enduring Freedom Library of Congress, Washington, DC (2207) Technical Report No. RS22452.
3. Warden D. Military TBI during the Iraq and Afghanistan wars. J Head Trauma Rehabil 21 (2006) 398-402.
4. Department of Defense Armed Forces Health Surveillance Center (AFHSC) 2011.
5. Moss W. C., King M. J. and Blackman G. Skull Flexure from Blast Waves: A mechanism for brain injury with implications for helmet design. Physical Review Letter 103 (2009).
6. Nyein M. K., Jason A. M., Yu L., Pita C. M., Joannopoulos J. D., Moore D. F., and Radovitzky R. A. In silico investigation of intracranial blast mitigation with relevance to military traumatic brain injury. In: Proc Natl Acad Sci USA 107(48) (2010) 20703-20708.
7. Grujicic M., Bell W., Pandurangan B., and Glomski P. S. Fluid/Structure interaction computational investigation of blast-wave mitigation efficacy of the advanced combat helmet. J. Materials Engineering and Performance 20(2010) 877.
8. Li J., Tan H. N. S., and Seng K. Y. A biomechanical computational study of the role of helmet pads in mitigating blast-induced traumatic brain injury. In: 6th World Congress of Biomechanics (WCB 2010): Magjarevic R, ed.: Springer Berlin Heidelberg (2010) 1518-1521.
9. Zhang L., Yang K. H., Dwarampudi R., Omori K., Li T., Chang K., Hardy W. N., Khalil T. B., and King A. I. Recent advances in brain injury research: a new human head model development and validation. Stapp Car Crash J 45(2001a) 369-394.
10. Sharma S., and Zhang L. Prediction of intracranial responses from blast induced neurotrauma using a validated finite element model of human head. In: Proceedings of Injury Biomechanics Symposium (IBS) (2011), Ohio State University.
11. Zhang L., Yang K. H., and King A. I. A proposed injury threshold for mild traumatic brain injury," J. Biomechanical Engineering 126(2004) 226-236.
12. Zhang L., Yang K. H., and Gennarelli T. A. Mathematical modeling of cerebral concussion: Correlations of regional brain strain with clinical symptoms. In: Proceedings of Biomechanics of Impact (IRCOBI) (2008)123-132.
13. Hardy W. N., Foster C. D., Mason M. J., Yang K. H., King A. I., and Tashman S. Investigation of head injury mechanisms using neutral density technology and high-speed biplanar X-ray. Stapp Car Crash J 45(2001) 337-368.
14. Nahum A. M., Smith R., and Ward C. C. Intracranial pressure dynamics during head impact. Proc. 21st Stapp Car Crash Conference (1977) 339-366.
15. Trosseille X., Tarriere C., Lavaste F., Guillon F., and Domont A. Development of a F.E.M. of the human head according to a specific test protocol. Proc. 36th Stapp Car Crash Conference (1992) SAE Paper No.922527.
16. Nyquist G. W., Cavanaugh J. M., Goldberg S. J., and King A. I. Facial impact tolerance and response. Proc. 30th Stapp Car Crash Conference (1986) SAE Paper No, 861896.
17. Allsop D. L., Warner C. Y., Wille M. G., Scheider D. C., and Nahum A. M. Facial impact response – A comparison of the Hybrid III dummy and human cadaver," Proc. 32nd Stapp Car Crash Conference (1988) SAE Paper No, 881719.
18. Hypermesh V10.0 Altair Hyperworks, 2010, Troy MI.
19. McEntire B. J., Whitley P., Blunt impact performance characteristics of the advanced combat helmet and the paratrooper and infantry personnel armor system for ground troops helmet. Fort Rucker, AL, U.S. Army Aeromedical Research Laboratory (2005) USAARL Report No. 2005-12.
20. Fallenstein G. T., Hulce V. D. and Melvin J. W. Dynamic mechanical properties of human brain tissue. J Biomechanics 2(1966) 217-226.
21. Galford J. E. and McElhaney J. H. Some viscoelastic study of scalp, brain and dura. ASME Paper No. 69-BHF-6 (1969) American Society of Mechanical Engineers, New York.
22. Moss W. C., King M. J. Impact response of U.S. Army and national football league and military helmet pads (2011) Report No. LLNL-SR-471496 DTIC ADA536266.
23. Hoof V. J., Duetekom M. J. Worswick M. J., and Bolduc M. Experimental and numerical analysis of the ballistic response of composite helmet materials. In: Proceedings of 18th International Symposium on ballistics (1999) San Anatonio, TX.

24. Aare M., and Kleiven S. Evaluation of head response to ballistic helmet impacts using the finite element method International J Impact Engineering 34(3) (2001) 596-608.
25. Team Wendy LLC, Cleveland OH
26. Leonardi A. D., Bir C. A., Ritzel D. V., and VandeVord P. J. Intracranial pressure increases during exposure to a shock wave. J Neurotrauma 28(2011) 85-94.
27. Zhu F., Mao H., Leonardi A. D., Wagner C., Chou C., Jin X., Bir C., VandeVord P., Yang K. H., and King A. I. Development of an FE Model of the Rat Head Subjected to Air Shock Loading. Stapp Car Crash J, 54 (2010) 211-225.
28. Wang J. Simulation of landmine explosion using LS-DYNA-3D software: Benchmark work of simulation of explosion in soil and air. Aeronautical and Maritime Research Laboratory (2001) DSTO-TR-1168.
29. Technical Manual Operator's Manual for Advanced Combat Helmet (ACH) (TM 108470-204-10) (2006) Gentex Corporation, Pennsylvania.
30. Zhang L., Sharma S., and Makwana R. Computational modeling of causal mechanisms of blast wave induced traumatic brain injury – a potential tool for injury prevention. *Technical Report* 2011 U.S. Army Medical Research and Materiel Command, Fort Detrick, Maryland 21702-5012.
31. Zhang L., Makwana R., and Sharma S. Comparison of the head response in blast insult with and without combat helmet. In: Proceedings of HFM-207 Symposium on Survey of Blast Injury across the Full Landscape of Military Science NATO OTAN Research & Technology Organisation (2011).
32. Sharma S. Biomechanical analysis of blast induced traumatic brain injury – a finite element modeling and validation study of blast effects on human brain (2011). *Wayne State University Theses*. Paper 138
33. Makwana R. Development and validation of a 3D FE model of advanced combat helmet and biomechanical analysis of human head and helmet response to blast insult (2012). *Wayne State University Theses.*
34. Zhang L., Yang K. H., and King A. I. Comparison of brain responses between frontal and lateral impact by finite element modeling. J Neurotrauma 18(2001b) 21-30.
35. Leonardi A. D. An investigation of the biomechanical response from shock wave loading to the head (January 1, 2011). *ETD Collection for Wayne State University.* Paper AAI3469965.